Analytic design and visualization of multiple surface plasmon resonance excitation using angular spectrum decomposition for a Gaussian input beam

Kyongsik Choi, Hwi Kim, Yongjun Lim, Seyoon Kim, and Byoungho Lee

School of Electrical Engineering, Seoul National University, Seoul 151-744, Korea
Phone: +82-2-880-7245, Fax: +82-2-873-9953
byoungho@snu.ac.kr

http://oeqelab.snu.ac.kr

Abstract: We propose an exact design, analysis, and visualization method for multiple surface plasmon resonance (MSPR) mode excitation phenomena for a structure composed of an optimized-thickness polymethyl-methacrylate layer and a gold thin-film layer. The proposed simulation method is based on a recursive transfer matrix method (R-TMM) and Gaussian angular spectrum decomposition. Our method illustrates, under the Kretchmann-Raether attenuated total reflection (ATR) geometry, the response for an angle-modulated Gaussian incident beam. To verify the simulation results we also performed experiments to excite MSPR modes under the ATR geometry. Our fast and exact R-TMM with the Gaussian angular spectrum method can be widely applied to the design and analysis of metal- and dielectric-composed thin film structures.

OCIS codes: (240.6680) Surface plasmons; (260.2110) Electromagnetic theory; (260.3910) Metals, optics of; (310.6860) Thin films, optical properties.

References and Links

1. H. Raether, *Surface Plasmons on Smooth and Rough Surfaces and on Gratings* (Springer-Verlag, Berlin, 1988).
2. A. V. Zayats, I. I. Smolyaninov, and A. A. Maradudin, "Nano-optics of surface plasmon polaritons," Phys. Reports **408**, 131-314 (2005).
3. J. Homola, S. Yee, and G. Gauglitz, "Surface plasmon resonance sensors: review," Sens. Actuators B **54**, 3-15 (1999).
4. B. Rothenhausler and W. Knoll, "Surface plasmon microscopy," *Nature* **332**, 615-617 (1988).
5. W. L. Barnes, A. Dereux, and T. W. Ebbesen, "Surface plasmon subwavelength optics," *Nature* **424**, 824-830 (2003).
6. P. Andrew and W. L. Barnes, "Energy transfer across a metal film mediated by surface plasmon polaritons," *Science* **306**, 1002-1005 (2004).
7. O. J. F. Martin, C. Girard, and A. Dereux, "Generalized field propagator for electromagnetic scattering and light confinement," Phys. Rev. Lett. **74**, 526-529 (1995).
8. C. Hafner, *The Generalized Multiple Multipole Technique for Computational Electromagnetics* (Artech House, Boston, 1990).
9. A. Taflove and S. C. Hagness, *Computational Electrodynamics: The Finite-Difference Time-Domain Method*, 2nd ed. (Artech House, Boston, 2000).
10. Y. Xie, A. R. Zakharian, J. V. Moloney, and M. Mansuripur, "Transmission of light through a periodic array of slits in a thick metallic film," Opt. Express **13,** 4485-4491 (2005), http://www.opticsexpress.org/abstract.cfm?URI=OPEX-13-12-4485.
11. P. Drude, "Zur Elektronentheorie der Metalle," Ann. Phys. **1**, 566-613 (1900).

#8867 - $15.00 USD Received 22 September 2005; revised 19 October 2005; accepted 18 October 2005

12. G. Mie, "Beiträge zur Optik trüber Medien, speziell Kolloidalen Metall-lösungen," Ann. Phys. **25**, 377–445 (1908).
13. *Handbook of Optical Constants of Solids*, edited by E. D. Palik (Academic, New York, 1985).
14. F.-C. Chien and S.-J. Chenb, "A sensitivity comparison of optical biosensors based on four different surface plasmon resonance modes," Biosensors and Bioelec. **20**, 633-642 (2004).
15. B. E. A. Saleh and M. C. Teich, *Fundamentals of Photonics* (John Wiley & Sons, New York, 1991).
16. F. I. Baida, D. V. Labeke, and J.-M. Vigoureux, "Near-field surface plasmon microscopy: A numerical study of plasmon excitation, propagation, and edge interaction using a three-dimensional Gaussian beam," Phys. Rev. B **60**, 7812-7815 (1999).
17. F. I. Baida, D. V. Labeke, and J.-M. Vigoureux, "Theoretical study of near-field surface plasmon excitation, propagation and diffraction," Opt. Commun. **171**, 317-331 (1999).

1. Introduction

Surface plasmon is an electromagnetic surface-bound wave (p-polarized, transverse-magnetic), propagating along the interface between metal and dielectric layers. The metal behaves like plasma, having equal amounts of positive and negative charges, of which the electrons are mobile. The bound wave has an evanescent field, which decays exponentially perpendicular to the surface. It can be produced by photons in the well-known Kretchmann-Raether attenuated total reflection (ATR) device. Surface plasmons have played a significant role in a variety of areas of fundamental and applied research [1, 2], from surface-sensitive sensors [3] to surface plasmon resonance microscopy [4], surface plasmon resonance technology [5], and a wide range of photonic applications [6].

There are several methods for numerically solving electromagnetism for any arbitrary geometry, such as the Green's function method [7], the multiple multipole technique [8], and the finite difference time domain (FDTD) technique [9, 10]. While the multiple multipole technique requires relatively little computational load, it requires a significant investment in user learning. The Green's function approach and FDTD require intensive computing load. However, our method proposed in this paper is very simple and fast and can exactly analyze the Gaussian beam response with small computing memory. In this work, we take the recursive transfer matrix method (R-TMM) approach with angular spectrum decomposition to analyze and visualize the excited multiple surface plasmon resonance (MSPR) phenomena on the gold (Au) thin-film layer with a polymethyl-methacrylate (PMMA) dielectric layer. For the MSPR modes excitation we coated a PMMA layer with the thickness of 450nm on an Au thin-film layer with the thickness of 30nm.

The rest of the paper is organized as follows: First, we describe analytical calculations for a simple three-layer surface plasmon resonance (SPR) structure with prism/Au/air layers. With its extension to multi-layer calculations, we analyze an MSPR phenomenon for our optimized four-layer structure with prism/Au/PMMA/air layers. Second, we propose and discuss the R-TMM under an oblique Gaussian beam input source condition using angular spectrum decomposition, and show some simulation results under the ATR geometry. And also, we compare the simulation results with the experimental results for the verification of the accuracy of our R-TMM method. Usually the SPR simulation has been done for uniform plane wave inputs. To our knowledge, this is the first time to propose an efficient method to analyze and visualize Gaussian input beam case. We especially discuss it with the MSPR structure – the topic which has not been much discussed yet.

2. Analytic solution of the SPR

The optical properties of metals have been of interest for at least 100 years [11]. Mie provided the form of the solution to the problem of light scattering by spherical metal particles in 1908 [12]. Other high-symmetry forms, including finite thickness slabs, cylinders, and ellipsoids, have been analytically solved. These analytical solutions require only the particle size and frequency-dependent complex index of refraction $\tilde{n} = n + ik$ with the real part representing

#8867 - $15.00 USD Received 22 September 2005; revised 19 October 2005; accepted 18 October 2005

the index of refraction and the imaginary part the absorption coefficient. These optical constants are available in the literature [13]. The surface plasmon has the propagation constant, k_{sp}, which can be determined by solving Maxwell's equations and continuity equations (boundary conditions) for an interface separating a metal from a dielectric with a p-polarized light. Following equations show the propagation constants and reflectivities.

$$k_x = \sqrt{\varepsilon_0}\frac{\omega}{c}\sin\theta = k_{sp} = \frac{\omega}{c}\sqrt{\frac{\varepsilon_1 \cdot \varepsilon_2}{\varepsilon_1 + \varepsilon_2}}, \quad k_{zi} = \sqrt{\varepsilon_i\left(\frac{\omega}{c}\right)^2 - k_x^2}, \quad (i = 1,2) \qquad (1)$$

where ε_1 and ε_2 are the complex dielectric constants of the prism and metal, respectively. θ is the incident angle of the probing light. Here k_{z2} is imaginary and the electric field distribution at the metal surface can be expressed by $E = E_0 e^{i(k_{x2}x - k_{z2}z - \omega t)}$ and its real amplitude distribution is given by $|E| = |E_0| e^{-|k_z|\cdot|z|}$. Hence the excited surface plasmons are exponentially decaying and the value of the skin depth, at which the magnitude of electric field falls to 1/*e* of its maximum, becomes $z_{skin} = 1/|k_{zi}|$.

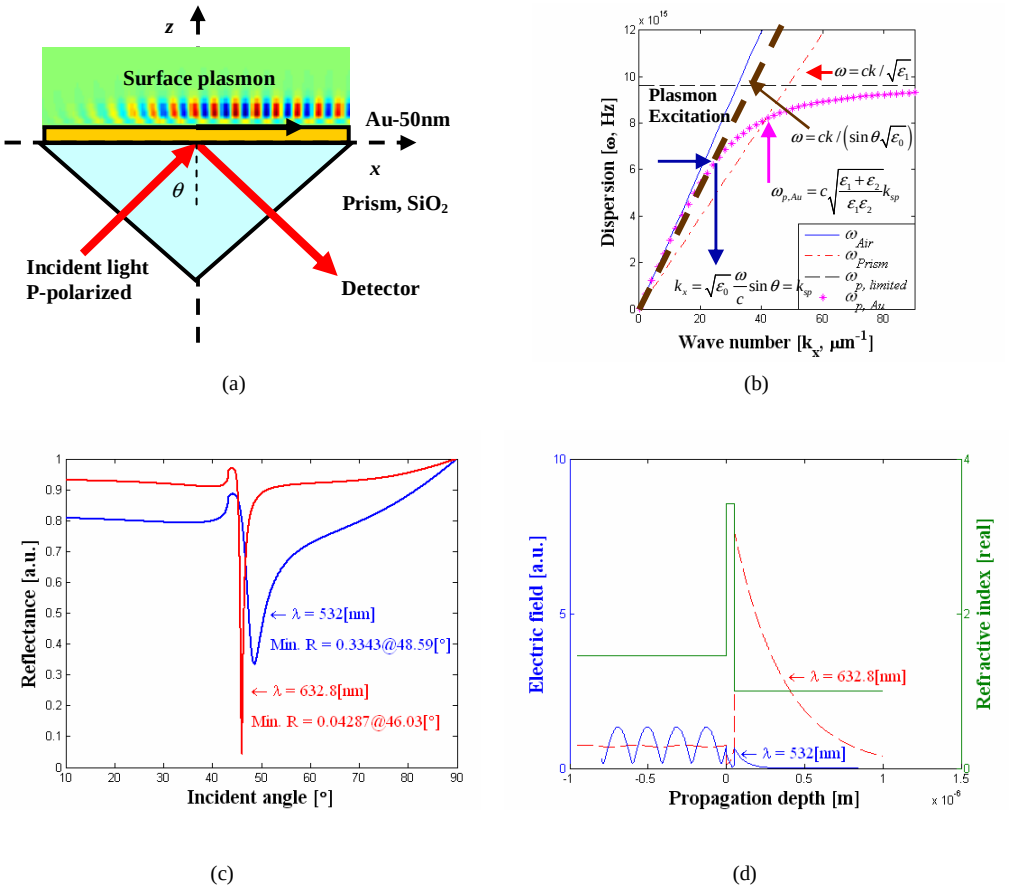

Fig. 1. (a) General Kretschmann-Raether's SPR structure and calculated (b) dispersion relation, (c) reflectance with respect to the incident angle variation, and (d) penetration depth with reconstruction wavelengths of 532nm and 632.8nm. The following parameters were used in the calculations: the refractive index of the substrate and SiO_2 prism is 1.460; the refractive index of the gold film is 0.402 + i2.540 @532nm, 0.1726 + i3.4218 @632.8nm, and its thickness is 50 nm. θ is the variable incident angle of the probing beam.

#8867 - $15.00 USD Received 22 September 2005; revised 19 October 2005; accepted 18 October 2005

From the Fresnel's equation we can calculate the reflectivity of the p-polarized incident light by the following equation.

$$R = \left| r_{012} \right|^2, \quad r_{012} = \frac{E_{ref}}{E_{inc}} = \frac{r_{01} + r_{12} e^{2i\delta}}{1 + r_{01} r_{12} e^{2i\delta}}, \quad r_{ij} = \left(\frac{k_{zi}}{\varepsilon_i} - \frac{k_{zj}}{\varepsilon_k} \right) \Big/ \left(\frac{k_{zi}}{\varepsilon_i} + \frac{k_{zj}}{\varepsilon_k} \right) \tag{2}$$

where, $\delta = k_{z2} d_2$ and d_2 is the thickness of the metal thin-film layer.

From these equations we can calculate the dispersion relation and reflectivity at a metal/dielectric interface. Figure 1 shows the general Kretchmann-Raether SPR structure with a gold surface and its dispersion relation, reflectance, and penetration depth. Figure 1(a) and (b) represent the basic ATR structure for SPR excitation and its dispersion relations for each layer. Figure 1(c) shows the calculated reflectance of the three-layer SPR structure with SiO_2 prism, Au film, and sample (air) layers using Eq. (2). Under the probing beams with the wavelength of 532nm and 632.8nm, we can obtain the minimum reflectivity of 0.3343 at the incident angle of 48.59° and 0.0429 at the incident angle of 46.03°, respectively. In addition, we can obtain the sharper dip under the wavelength of 632.8nm than the wavelength of 532nm. This means that one can obtain the better sensitivity and long penetration distance under the wavelength of 632nm but it needs more angular resolution. From Fig. 1(d) we can see the propagation distance of the evanescent wave generated by the excited SPR on the Au thin film layer. In this figure, we assumed the input source is a sinusoidal plane wave. From the result, we can see that the strongly excited SPR decays exponentially along the surface normal direction under the wavelength of 632.8nm. And also, we can get the penetration distance about 0.425μm under the wavelength of 632.8nm.

Equation (2) for a three-layer structure can be easily extended to a four-layer equation by replacing r_{12} with r_{123} which has the same form as r_{012} in Eq. (2) with the appropriate indices. Hence, by continuing this recursive procedure the reflectance for an arbitrary number of layers can be found and simply represented by multiple scattering matrix form. The tangential fields at the first boundary $z = z_1 = 0$ are related to those at the final boundary $z = z_{N-1}$ by

$$\begin{bmatrix} U_1 \\ V_1 \end{bmatrix} = M_2 M_3 \ldots M_{N-1} \begin{bmatrix} U_{N-1} \\ V_{N-1} \end{bmatrix} = \prod_{k=2}^{N-1} M_k \begin{bmatrix} U_{N-1} \\ V_{N-1} \end{bmatrix}, \tag{3}$$

where, $M_k = \begin{bmatrix} \cos\beta_k & -i \sin\beta_k / q_k \\ -i q_k \sin\beta_k & \cos\beta_k \end{bmatrix}$ and $q_k = \left(u_k / \tilde{\varepsilon}_k \right)^{1/2} \cos\theta_k$. If we assume the metal has no magnetic loss component, then $u_k \cong 1$ and $q_k = \left(1/\tilde{\varepsilon}_k \right)^{1/2} \cos\theta_k = \left(\tilde{\varepsilon}_k - n_1^2 \sin^2\theta_1 \right)^{1/2} / \tilde{\varepsilon}_k$, and β_k is given by $\beta_k = \left(2\pi/\lambda \right) \tilde{n}_k \cos\theta_k \left(z_k - z_{k-1} \right) = \left(z_k - z_{k-1} \right) \left(2\pi/\lambda \right) \left(\tilde{\varepsilon}_k - n_1^2 \sin^2\theta_1 \right)^{1/2}$. For p-wave at boundary *k*, $U_k = H_y^T + H_y^R$, $V_k = E_z^T + E_z^R$ and the reflection and transmission coefficients for p-wave can be calculated by following equations:

$$R_p = \left| r_p \right|^2, \quad r^p = \frac{\left(M_{11} + M_{12} q_N \right) q_1 - \left(M_{21} + M_{22} q_N \right)}{\left(M_{11} + M_{12} q_N \right) q_1 + \left(M_{21} + M_{22} q_N \right)},$$

$$M_{ij} = \left(\prod_{k=2}^{N-1} M_k \right)_{ij}, \quad i, j = 1, 2, \cdots \tag{4}$$

#8867 - $15.00 USD Received 22 September 2005; revised 19 October 2005; accepted 18 October 2005

Figure 2(a) shows our multi-layered MSPR structure composed of a SiO_2 prism and slide glass, Cr and Au, and PMMA layers. This structure has been optimized for MSPR excitation. The slide glass with the thickness of 500 μm is used as a buffer layer for index matching with the prism. The Cr layer with the thickness of 1nm is added for good adhesion between SiO_2 and the Au layer. The dispersion relation, reflection profile, and penetration depth profile are presented at Figs. 2(b), 2(c), and 2(d).

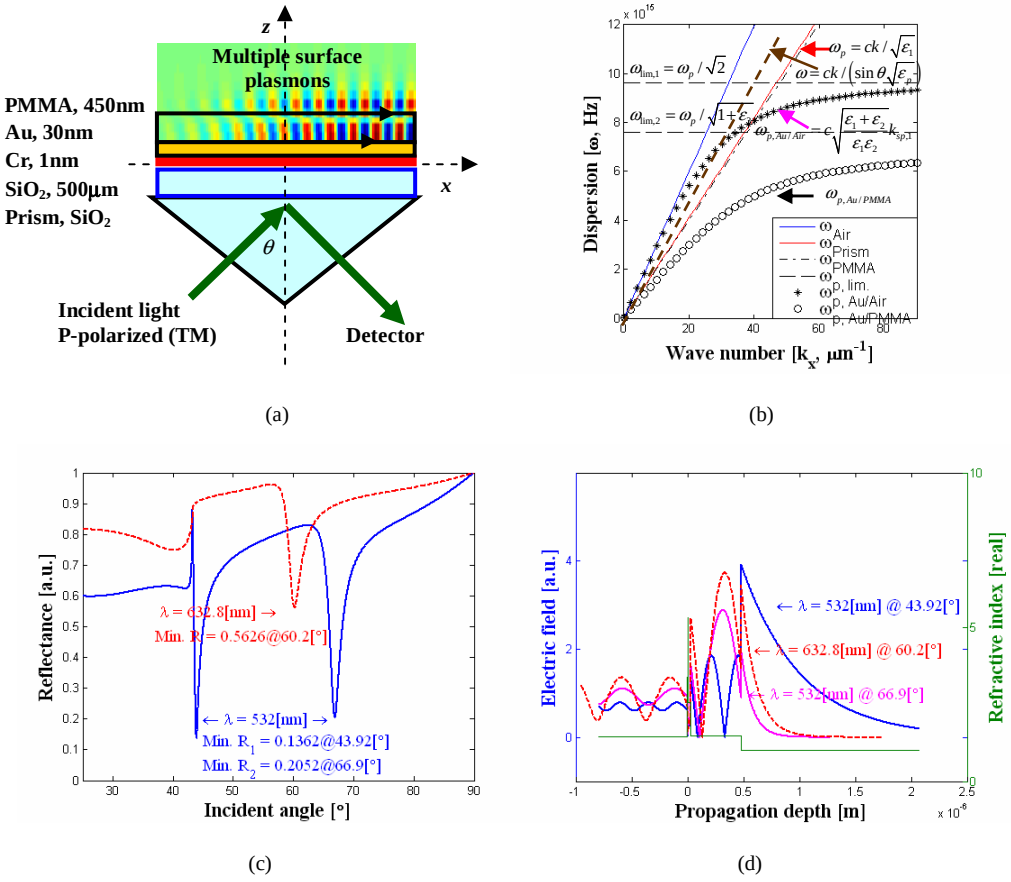

Fig. 2. (a) Proposed multiple SPR sensor structure and calculated (b) dispersion relation, (c) reflectance with respect to the incident angle variation, and (d) penetration depth with two different reconstruction wavelengths of 532nm and 632.8nm. The following parameters were used in the calculations: the refractive index of the substrate and SiO_2 prism is 1.460; the refractive index of the Cr film is 2.9 + i4.44 at the wavelength of 532nm, 1.44 + i3.40 at the wavelength of 632.8nm and its thickness is 1nm; the refractive index of the Au film is 0.402 + i2.540 at the wavelength of 532nm, 0.1726 + i3.4218 at the wavelength of 632.8nm, and its thickness is 30nm; the refractive index and the thickness of the PMMA layer are 1.490 and 450nm, respectively.

As shown in Fig. 2(c), we can get the two minima reflectance (modes) of 0.2497 at the angle of 43.89° and 0.2604 at the angle of 66.79° under the probing beam with the wavelength of 532nm. The former mode is a waveguide-coupled (WC) SPR mode and the latter is the SPR mode [3, 14]. However, only one minimum peak is observed at the wavelength of 632.8nm. To obtain these uniform multiple minima absorption peaks requires some careful configurations of the thicknesses of metal layer and dielectric layers such as organic polymer (PMMA, photo-resist) and glass (silica, borosilicate, flint, crown). For MSPR modes excitation, we optimized a PMMA layer with the thickness of 450nm and an Au layer with the

#8867 - $15.00 USD Received 22 September 2005; revised 19 October 2005; accepted 18 October 2005

thickness of 30nm. Figure 2(d) shows the propagation distance of the evanescent wave and its guided mode profiles. We can see that the two absorption peaks (modes) exist in the PMMA layer at the wavelength of 532nm but only one mode appears at the wavelength of 632.8nm.

3. R-TMM visualization with a Gaussian angular spectrum decomposition method

In this section we discuss how to calculate the propagation of beams with the R-TMM method under an oblique Gaussian beam incidence condition. The Maxwell's equations are decoupled into two polarization sets; the TM set $E_x H_y E_z$ and the TE set $H_x E_y H_z$. Each field set can be modeled independently of the other. Solving the Maxwell equations considering boundary conditions of the SPR structure, the electric and magnetic fields distribution at the *i-th* layer under the TM (p-polarized) incident beam can be expressed as the following equation:

$$H_i = \frac{k_0 n_i}{\omega \mu_0}\left\{M_{i,11}\exp\left[ik_{zi}\left(z-l_{i-1}\right)\right]+M_{i,12}\exp\left[-ik_{zi}\left(z-l_{i-1}\right)\right]\right\}\exp\left(ik_{xi}x\right),$$

$$E_i = \frac{k_{zi}}{k_0 n_i}\left\{M_{i,11}\exp\left[ik_{zi}\left(z-l_{i-1}\right)\right]-M_{i,12}\exp\left[-ik_{zi}\left(z-l_{i-1}\right)\right]\right\}\exp\left(ik_{xi}x\right), \quad (5)$$

where $l_i = \sum_{k=0}^{i} d_i$ for $0 \le i \le N$, $d_0 = 0$, and d_i is the thickness of the *i-th* layer. Now we consider the propagation of an incident Gaussian beam, i.e. incident TM field $E(x,z)$ that is not a uniform plane wave. In particular we will discuss the propagation of the fundamental Gaussian beam. The Gaussian beam is the ideal diffraction limited wave and often approximates laser beams well. Equation (6) shows the complex amplitude $U(x,z)$ of the Gaussian beam [15-17].

$$U\left(x,z\right) = E_0 \frac{w_0}{w\left(z\right)}\exp\left[-\frac{x^2}{w^2\left(z\right)}\right]\exp\left[-j\left(kz + k\frac{x^2}{2R\left(z\right)} - \zeta\left(z\right)\right)\right], \quad (6)$$

where $w\left(z\right) = w_0\left[1+\left(z_0/z\right)^2\right]^{1/2}$ is the beam width, $R\left(z\right) = z\left[1+\left(z_0/z\right)^2\right]$ is the wavefront radius of curvature, $\zeta\left(z\right) = \tan^{-1}\left(z/z_0\right)$, $z_0 = k_0 w_0^2$ is the Rayleigh range, and $w_0 = \left(\lambda z_0/\pi\right)^{1/2}$. We assume the incident field at a plane $z=0$ has the Gaussian beam profile. A multilayered stack extends form $z=0$ to $z=L$. We can calculate the field directly at all positions using the R-TMM method. For linear, space-invariant systems, the input field can be decomposed into elementary components. Hence these can be propagated individually, and the output field is obtained by summing the propagated individual components. One possible decomposition method of the incident field $E(x, z=0)$ is obtained by performing the spatial Fourier transform given by Eq. (7).

$$A\left(f_x; z=0\right) = \int_{-\infty}^{\infty} E\left(x, z=0\right)\exp\left[-i2\pi f_x x\right]dx. \quad (7)$$

The inverse Fourier transform of Eq. (7) expresses the field as a function of the Fourier components $A\left(f_x; z=0\right)$.

$$E\left(x, z=0\right) = \int_{-\infty}^{\infty} A\left(f_x; z=0\right)\exp\left[i2\pi f_x x\right]df_x. \quad (8)$$

#8867 - $15.00 USD Received 22 September 2005; revised 19 October 2005; accepted 18 October 2005

Comparing the integrand of Eq. (8) with the equation for a plane wave $E(x,z)=E(x,0)\exp(ik_0 z)$, we see that the Fourier transform decomposes the E-field into plane waves with amplitudes $A(f_x;z=0)$ and wavevectors $k_x=2\pi f_x$ in the *x*-direction. The spatial frequency f_x is related to the directional cosine α, $f_x=\alpha/\lambda$. Thus we see that the integration in Eq. (8) corresponds to the summation of plane waves with amplitudes $A(f_x;z=0)$ propagating in different directions in the *x*-*z* plane. We can calculate the change of the plane wave amplitude $A(f_x;z=0)$ as a function of z using the proposed R-TMM. The transfer function relating $A(f_x;z)$ to $A(f_x;0)$ is obtained from M_k's in Eq. (3). Due to the discrete nature of the Fourier transform, the resulting E-field is repetitive in space. The repetition distance is $\Delta x=\lambda/\Delta\alpha$, where $\Delta\alpha$ is the minimum required angular sampling distance. If the E-field of interest is limited in space or can be approximated by a spatially limited function extending over a spatial distance smaller than Δx, the discrete Fourier transform combined with a spatial filter of width Δx correctly reconstructs the original field. Figure 3 shows the R-TMM visualization of the excited MSPR phenomena under the oblique Gaussian beam input.

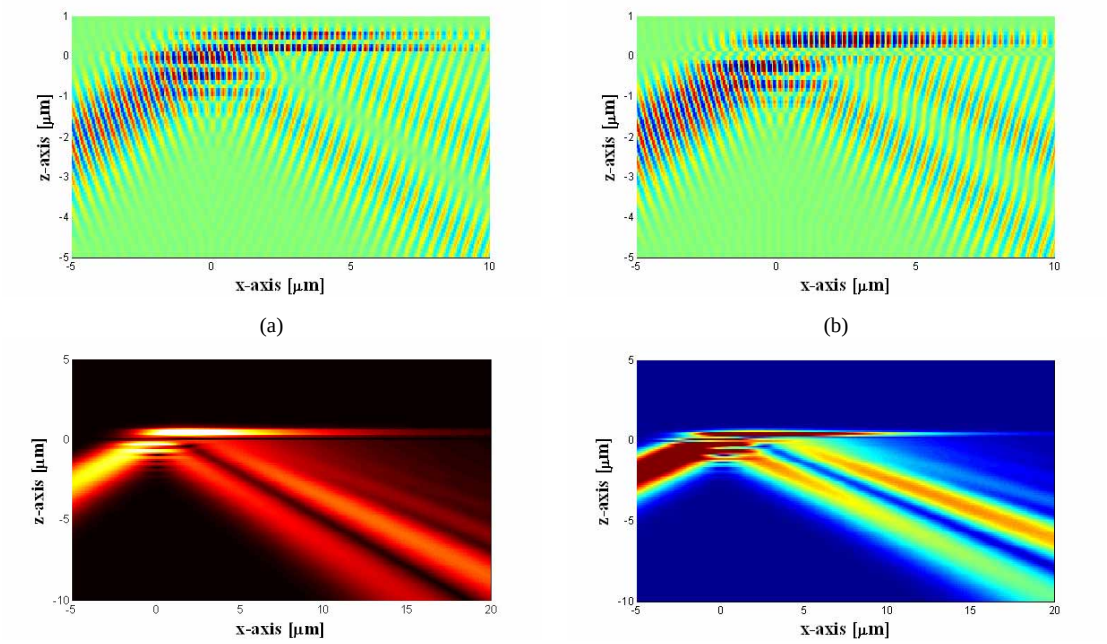

Fig. 3. Simulation results for MSPR excitation phenomena for the structure with four-layer (prism/Au/PMMA/air) using the proposed R-TMM with Gaussian angular spectrum decomposition method; (a) E_x–field and (b) E_z–field distribution of our proposed MSPR structure under the incident angle of 66.8° with the wavelength of 532 nm, (c) simulated movie for MSPR excitation with respect to the angle modulation for the Gaussian beam input with the wavelength of 632.8 nm, and (d) simulated movie for MSPR excitation with respect to the angle modulation for the Gaussian beam input with the wavelength of 532 nm.

Figure 3 shows the simulation results for MSPR excitation phenomena using our proposed R-TMM under the oblique Gaussian incident beam condition with four layers

#8867 - $15.00 USD Received 22 September 2005; revised 19 October 2005; accepted 18 October 2005

(prism/Au/PMMA/air). From Fig. 3(a) we can see that the multiple plasmon modes have been generated and propagated evanescently toward *x*-direction not only on the metal but also on the PMMA surface. The WC-SPR mode excited at the angle of 43.92° has higher amplitude and sharper bandwidth characteristics than the SPR mode excited at the angle of 66.9°. This means that the WC-SPR mode has higher sensitivity under the small angle (or wavelength) interrogation. From these figures we can see that all the transmitted waves through the Au layer have exponentially decaying characteristics along both the *x*- and *z*-directions. Figure 3(b) shows the E_z field distribution and the penetration depth of about 0.4μm for the wavelength of 532nm. Figures 3(c) and 3(d) show the MSPR simulation results with the four-layer structure under the angle-modulated Gaussian incident beam with the wavelength 632.8nm and 532nm, respectively. From Fig. 3(d) we can see that two minima absorption peaks are generated at the angle of 43.92° and 66.9°, respectively. In our simulation we used a personal computer with Pentium4 3GHz CPU machine. A fast calculation time about 60.11 seconds per frame was achieved. The frame size is 500×150 and the minimum angular sampling rate $\Delta\alpha$ is 0.02°.

4. Experimental results and discussion

The SPR detection system can be implemented by the most common Kretschmann-Raether ATR coupling system, in which a thin metal film is attached to a prism with a relatively high refractive index. The light then passes through the prism, at an angle of incidence greater than the critical angle for the prism, which means that total reflection occurs at the prism-metal interface. At total reflection, an evanescent field is induced, which is able to penetrate to the metal film and excites a surface plasmon wave at the metal-ambient interface. Figure 4(a) shows our ATR coupling system combined with a LabView control system and Fig. 4(b) shows the experimental results from our multiple SPR excitation structure using two probing lights with the wavelength of 532nm (DPSS Nd:YAG laser) and 632.8nm (HeNe laser). From the result we can see that the theoretical and experimental results are almost matched together. Utilizing this setup, both angular and wavelength interrogations are possible.

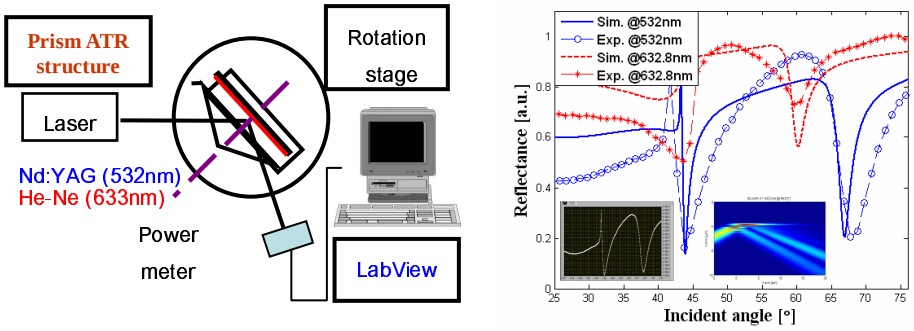

(a) (b)

Fig. 4. (a) Kretchmann-Raether ATR coupling system and (b) its experimental result.

5. Conclusions

We presented an exact design, analysis, and visualization method for MSPR excitation phenomena for a structure composed of a PMMA layer and an Au thin-film using the R-TMM under an oblique Gaussian incident beam condition. And also, we fabricated and analyzed a PMMA-based MSPR structure with the optimized thicknesses of Au and PMMA layers. The proposed R-TMM illustrated, under the Kretchmann-Raether ATR geometry, the response for an angle-modulated Gaussian incident beam. The proposed R-TMM result matches well with

#8867 - $15.00 USD Received 22 September 2005; revised 19 October 2005; accepted 18 October 2005

the experimentally obtained result in our MSPR structure as shown in Fig. 4. Our proposed fast and exact R-TMM with Gaussian angular spectrum decomposition method can be widely applied to metal and dielectric composed thin-film structure design and analysis. And also, it has potentials for multiple bio-sensing, simultaneous thin-film thickness and refractive index measurement, and nano-photonics applications with careful structure designs in accordance with specific applications.

#8867 - $15.00 USD Received 22 September 2005; revised 19 October 2005; accepted 18 October 2005